# Population kinetics on $K\alpha$ lines of partially ionized Cl atoms

Tohru Kawamura,[1,*] Hiroaki Nishimura,[1] Fumihiro Koike,[2] Yoshihiro Ochi,[1] Ryoji Matsui,[1] Wen Yong Miao,[3] Shinichiro Okihara,[1] Shuji Sakabe,[1] Ingo Uschmann,[4] Eckhart Förster,[4] and Kunioki Mima[1]

[1]*Institute of Laser Engineering, Osaka University, 2-6 Yamada-Oka, Suita, Osaka 565-0871, Japan*

[2]*Information Networking Center, Kitasato University, Kitasato 1-15-1, Sagamihara, Kanagawa 228-8555, Japan*

[3]*Southwest Institute of Nuclear Physics and Chemistry, P.O. Box 919-216, Mianyang 621900, Sichuan, People's Republic of China*

[4]*X-ray Optics Group, Institute of Optics and Quantum Electronics, Friedrich-Schiller University Jena, Max-Wien-Platz 1, 07743, Jena, Germany*

(Received 14 November 2001; published 12 July 2002)

A population kinetics code was developed to analyze $K\alpha$ emission from partially ionized chlorine atoms in hydrocarbon plasmas. Atomic processes are solved under collisional-radiative equilibrium for two-temperature plasmas. It is shown that the fast electrons dominantly contribute to ionize the *K*-shell bound electrons (i.e., inner-shell ionization) and the cold electrons to the outer-shell bound ones. Ratios of $K\alpha$ lines of partially ionized atoms are presented as a function of cold-electron temperature. The model was validated by observation of the $K\alpha$ lines from a chlorinated plastic target irradiated with 1 TW Ti:sapphire laser pulses at $1.5\times10^{17}$ W/cm$^2$, inferring a plasma temperature of about 100 eV on the target surface.

DOI: 10.1103/PhysRevE.66.016402 PACS number(s): 52.25.Jm, 52.50.Jm, 52.70.La, 32.70.−n

## I. INTRODUCTION

The physics of ultrashort laser pulses with dense plasma interaction is of wide interest because of its close relevance to challenging researches on femtosecond x-ray radiation probing [1], energetic particle accelerations [2], and inertial confinement fusion (ICF) [3]. In the experiments, *K*-shell line spectroscopy is one of the standard diagnostics of hot dense plasmas. Line radiation from highly ionized tracers, such as those from hydrogenlike and/or heliumlike Ar and their satellite lines, are used to deduce temperatures and densities of compressed plasmas [4–6]. Properties of higher-order satellite lines [$Ar^{15+}:1s^2nl'-1s3lnl'(n=4,5,6)$] were studied theoretically to examine their contribution to corresponding He$\beta$ [7–10]. In relevance to the fast ignition approach to ICF [3], it has been shown that $K\alpha$ emission is a useful diagnostic medium for energetic electrons [11,12]. In contrast to this approach, measurement of x-ray absorption and/or emission from partially ionized plasmas is also useful, particularly for dense but low-temperature plasmas. Chenais-Popovics *et al.* studied the absorption spectroscopy of partially ionized Al and Cl $K\alpha$ lines [13]. They measured absorption spectra of these lines and analyzed them numerically with the use of a one-dimensional Lagrangian code combining an average-atom model for population calculations. In that work, they also developed a detailed collisional-radiative model. This model was, however, applicable only to the atomic ground state and the first two resonance levels for $1s^2(2s+2p)^N$ $(N=0-7)$. Burnett *et al.* [14] and Rousse *et al.* [15] measured Al $K\alpha$ spectra, and found that fast electrons carried about 10% of the incident laser energy. In their studies, Burnett *et al.* used a time evolution of the $K\alpha$ yield from $Al^{7+}$, and Rousse *et al.* ratios for the $K\alpha$ emission of $Al^{5+}$ to cold $K\alpha$.

As described above, $K\alpha$ emission from partially ionized atoms is expected to be useful for the investigation of not only fast-electron properties but also cold bulk-electron ones. Outer-shell bound electrons of atoms are collisionally ionized mostly by bulk electrons, and inner-shell bound ones by fast electrons. Consequently, the resultant $K\alpha$ emission can be seen between the primary $K\alpha$ and corresponding He$\alpha$ lines. Energetic electrons propagate in a cold dense region and deposit their energy to the bulk plasma. In this case, electrons with approximately two different temperatures exist in the plasma. The idea of a non-Maxwellian distribution has long been considered [16,17]. A numerical code has been developed for the study of Al $K\alpha$ emission by MacFarlane *et al.* [18], but that was for intense proton beams, and free electrons of a single Maxwellian distribution were assumed.

In this study, we developed a population kinetics code with a bi-Maxwellian temperature distribution. It is shown that $K\alpha$ emission is available to diagnose cold plasma temperature. After describing the model adopted in the code, we will show a simple analysis of experimentally obtained $K\alpha$ emission.

## II. $K\alpha$ LINES FROM PARTIALLY IONIZED ATOMS

The emission energies and radiative decay rates were obtained with the use of a multiconfiguration Dirac-Fock atomic code GRASP [19]. Figure 1 shows the resultant radiative decay rates of $K\alpha$ lines from various ionization states of Cl atoms. For $Cl^{1+}-Cl^{13+}$, we considered the $K\alpha$ transitions assuming their outermost bound electrons are not excited (namely, $Cl^{1+}:1s2s^22p^63s^23p^5 \rightarrow 1s^22s^22p^53s^23p^5$, . . . , $Cl^{13+}:1s2s^22p\rightarrow 1s^22s^2$). For $Cl^{14+}$, only transitions associated with $1s2s2p$ state were considered. The primary $K\alpha$ ($Cl^+$) transitions are distributed in the range of about 2622–2628 eV. Energy differences from the primary $K\alpha$ can be seen according to respective

*Present address: Gesellschaft für Schwerionenforschung, Planckstrasse 1, D-64291 Darmstadt, Germany; FAX: +49-(0)6159-713714; email address: t.kawamura@gsi.de

 

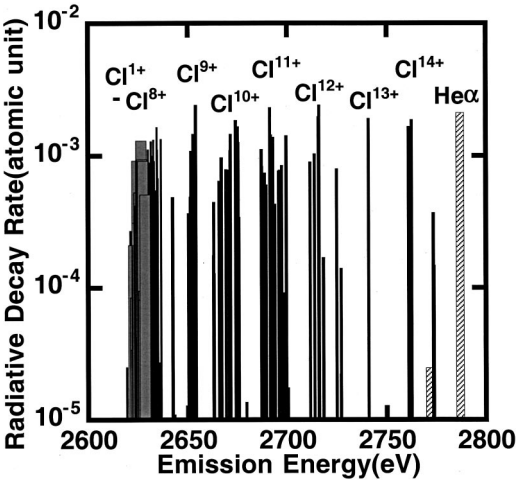


FIG. 1. Radiative decay rates for the $K\alpha$ lines of Cl atoms calculated by GRASP. The hatched bars on the left-hand side show primary $K\alpha$ ($Cl^{+}$).

charge states. The $K\alpha$ lines from He-like to O-like Cl are well separated from the primary ones, and those from Ne-like to S-like Cl are merging into each other. The $K\alpha$ lines of F-like Cl make a wing of the primary ones in the blue side.

To estimate the net intensity of $K\alpha$ emission, Auger transitions are very important, since $K\alpha$ emission is affected by the competition between radiative and Auger processes. Calculation of Auger rates was done with the use of an atomic code developed by Fritzsche *et al.* [20]. In Fig. 2, calculated Auger rates and the corresponding fluorescence yields of $K\alpha$ emission are given. The *KLL*-Auger is the most predominant process of all Auger transitions because electron correlation within the *L* shell is very effective. It is found that the fluorescence yields for $Cl^{+}-Cl^{13+}$ are about 0.1. They have more Auger channels than the autoionization state of $Cl^{14+}$ $(1s2s2p)$, for which fluorescence yield is about 0.5.

### III. DESCRIPTIONS OF AN ATOMIC MODEL

The free-electron distribution $F(E)_{\mathrm{All}}$ is assumed to be a bi-Maxwellian distribution consisting of the cold bulk component $F(E)_{\mathrm{bulk}}$, and the high temperature one $F(E)_{\mathrm{fast}}$,

$$F(E)_{\mathrm{all}}=(1-h)F(E)_{\mathrm{bulk}}+hF(E)_{\mathrm{fast}}, \tag{1}$$

where $h$ stands for a fraction of fast electrons, namely, $h=N_{e\mathrm{fast}}/(N_{e\mathrm{fast}}+N_{e\mathrm{bulk}})$, where $N_{e\mathrm{fast}}$ is a density of fast electrons and $N_{e\mathrm{Bulk}}$ is that of cold electrons. Cold electrons in bulk plasma play a role in outer-shell ionization, and fast electrons mainly in the *K*-shell ionization.

Except Auger $A_a$ and radiative decay $A_r$ for miscellaneous atomic transitions, rate coefficients are composed of two free-electron components. In the framework of a bi-Maxwellian distribution, effective rate coefficients $\mathcal{R}_{\mathrm{eff}}$ are obtained as follows [16,21,22]:

$$\mathcal{R}_{\mathrm{eff}}=(1-h)\mathcal{R}_{\mathrm{bulk}}+h\mathcal{R}_{\mathrm{fast}}\ \ (1/\mathrm{sec}), \tag{2}$$

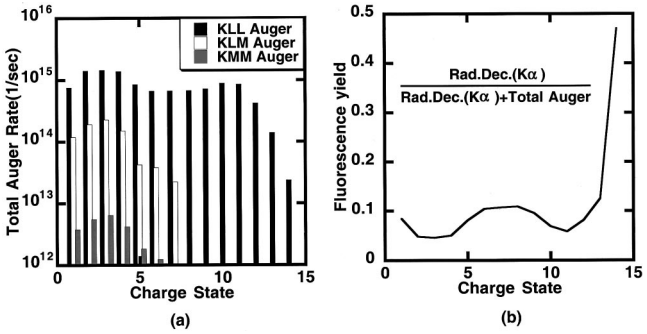


FIG. 2. Atomic features of partially ionized Cl atoms. (a) Auger transition rates and (b) fluorescence yield of respective $K\alpha$ lines.

where $\mathcal{R}_{\mathrm{eff}}$ means any of rate coefficients for collisional excitation/deexcitation $C_{\mathrm{eff}}/D_{\mathrm{eff}}$, collisional ionization $I_{\mathrm{eff}}$, inner-shell ionization $I_{\mathrm{eff}}^{\mathrm{inner}}$, radiative recombination $\mathcal{R}_{\mathrm{eff}}^{r}$, or dielectronic recombination $\mathcal{R}_{\mathrm{eff}}^{d}$. In the case of three-body recombination $\mathcal{R}_{\mathrm{eff}}^{3b}$, however, two free electrons have to be taken into consideration. According to Ref. [23], the three-body recombination rate for an arbitrary electron energy distribution $f(E)$ was obtained as follows:

$$\mathcal{R}_{\mathrm{eff}}^{3b}(z,i)=N_e^2\frac{h^3}{8\pi m_e^2}\frac{g_{z,i}}{g_{z+1,j}}\xi_{z,i}\int_{I_{nl}^{p'}}^{\infty}\sigma_{z,i}(E_1)\times\int_0^{E_1-I_{nl}^{p'}}\frac{f(E_2)f(E_1-E_2-I_{nl}^{p'})}{E_2^{1/2}(E_1-E_2-I_{nl}^{p'})^{1/2}}\times dE_2dE_1(1/\mathrm{sec}), \tag{3}$$

where $N_e$ is a total electron density, $\xi_{z,i}$ is the number of equivalent bound electrons in the $i$th shell in a state with lowered ionization potential $I_{nl}^{p'}$, $g_{z,i}$ and $g_{z+1,j}$ are the degeneracy of a state after/before recombination, and $\sigma_{z,i}(E)$ stands for the collisional ionization cross-section of level $i$ in a charge state $z$. For $\sigma_{z,i}(E)$, we adopted a formula that can be obtained from Ref. [24],

$$\sigma_{z,i}(E)=\frac{Q^R(E)}{(I_{nl}^{p'}/I_H)^2\left\{1+\dfrac{1}{1+[\log_{10}(E/I_{nl}^{p'})]^2}\right\}}\times 10^{-16}(\mathrm{cm}^2), \tag{4}$$

where

$$Q^R(E)=2.284\frac{\ln(E/I_{nl}^{p'})}{E/I_{nl}^{p'}}+2.023\frac{(E/I_{nl}^{p'})-1}{(E/I_{nl}^{p'})^2}-1.699\frac{(E/I_{nl}^{p'})-1}{(E/I_{nl}^{p'})^3}(\mathrm{cm}^2). \tag{5}$$

For the inner-shell ionization rates of the *K*-shell bound electrons, the formula derived by Sampson *et al.* [25–27] was adopted,

$$I^{\text{inner}}(nl)=N_e\pi\alpha_0^2\left(\frac{8T_e}{\pi m_e}\right)^{1/2}\left(\frac{n}{Z_{\text{eff}}(nl)S_0}\right)^4\xi_{z,nl}y[S_0^2D(nl)\exp(-y)-S_0yd(nl)E_3(y)$$
$$+\{A(nl)+S_0y[c(nl)-2S_0D(nl)]\}E_1(y)+S_0y\{S_0D(nl)+d(nl)-c(nl)\}E_2(y)](1/\text{sec}), \quad (6)$$

where

$$y=I_{nl}^{p'}/T_e, \quad (7)$$

$$S_0=I_{nl}^{p'}/I_{nl}^{p}. \quad (8)$$

$I_{nl}^{p}$ stands for the ionization potential of an isolated atom, $\alpha_0$ is the Bohr radius, and $E_n(y)$ is an exponential integral. The empirical coefficients $A(nl)$, $D(nl)$, $c(nl)$, and $d(nl)$ for each $nl$ orbital in the above formula can also be obtained from their papers. The effective charge $Z_{\text{eff}}(nl)$ for a bound electron in $nl$ orbital up to $n=6$ can be estimated from their relevant work [28,29]. The other rate coefficients for the outermost bound electrons of the atomic states considered here can be found in Ref. [7].

Figure 3 shows the model of population kinetics treated in this paper. In this model, since the fraction of fast electrons is expected to be very small compared with that of bulk ones, populations of $1s$-holed ions are assumed to be small. Therefore, the atomic transitions from these atoms to the corresponding ground states or singly excited states may be negligible when the populations of ground states or singly excited states are estimated. Namely, the rate equation can be separated into two blocks,

$$\frac{dN(z,i)}{dt}=\sum_{j(<i)}C_{\text{eff}}(j\rightarrow i)N(z,j)+\sum_{j(>i)}\{D_{\text{eff}}(j\rightarrow i)+A_r(j\rightarrow i)\}N(z,j)$$
$$-\left[\sum_{j(>i)}C_{\text{eff}}(i\rightarrow j)+\sum_{j(<i)}D_{\text{eff}}(i\rightarrow j)+\sum_{j(<i)}A_r(i\rightarrow j)\right]N(z,i)-I_{\text{eff}}(z,i)N(z,i)+\mathcal{R}^{\text{all}}(z,i)N(z+1,1)$$
$$-I_{\text{eff}}^{\text{inner}}(z,i)N(z,i)\delta_{1,i}+\sum_j\{I_{\text{eff}}(z-1,j)N(z-1,j)-\mathcal{R}^{\text{all}}(z-1,j)N(z,1)\}\delta_{1,i}=0, \quad (9)$$

where the atomic transitions from $1s$-holed ions are neglected. This equation was solved in the framework of the algorithm published by Lee [30]. In the above formula, $\mathcal{R}^{\text{all}}(z,i)$ includes three body, radiative, and dielectronic recombinations. The atomic energy levels for singly excited states up to principal quantum number $n=10$ were considered. Binding energy of the outermost bound electron is estimated with the use of the screened hydrogenic model, including $l$ splitting developed by Perrot [31]. The other oscillator strengths, except those associated with $K\alpha$ transitions, are based on a formula in Ref. [32].

The rate equation for the ground states of $1s$-holed ions $N^*(z,1)$ may be described as follows:

$$\frac{dN^*(z,1)}{dt}=I_{\text{eff}}^{\text{inner}}(z-1,1)N(z-1,1)-(A_r^{K\alpha}+A_a)N^*(z,1)-I_{\text{eff}}(z,1)N^*(z,1)+\{\mathcal{R}_{\text{eff}}^{3b}(z,1)+\mathcal{R}_{\text{eff}}^{r}(z,1)\}N^*(z+1,1)$$
$$+I_{\text{eff}}(z-1,1)N^*(z-1,1)-\{R_{\text{eff}}^{3b}(z-1,1)+R_{\text{eff}}^{r}(z-1,1)\}N^*(z,1)=0, \quad (10)$$

where $A_r^{K\alpha}$ means a radiative decay rate accompanied with $K\alpha$ emission, and $A_a$ stands for an Auger decay rate. In population calculations, split sublevels associated with a total angular momentum quantum number $J$ are combined together and are treated as a degenerate single level. When we use resultant populations for evaluating $K\alpha$ intensities in the framework of GRASP, the populations of each sublevel are determined by LTE, i.e., the Boltzmann distribution.

## IV. NUMERICAL SIMULATIONS

In this section, we demonstrate availability of $K\alpha$ emission by some numerical model calculations under collisional-radiative equilibrium (CRE).

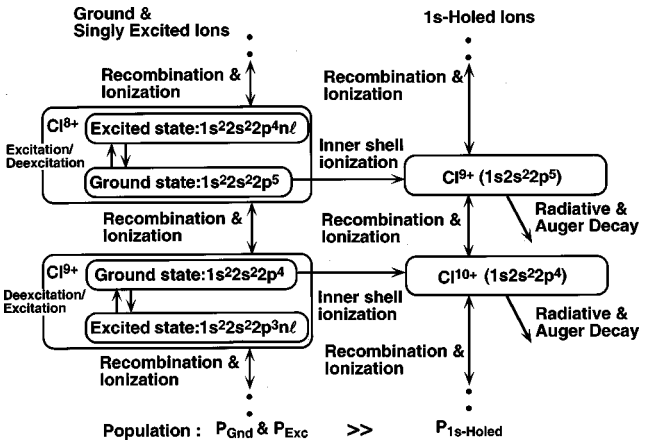


FIG. 3. Model of the population kinetics for 1*s*-holed atoms.

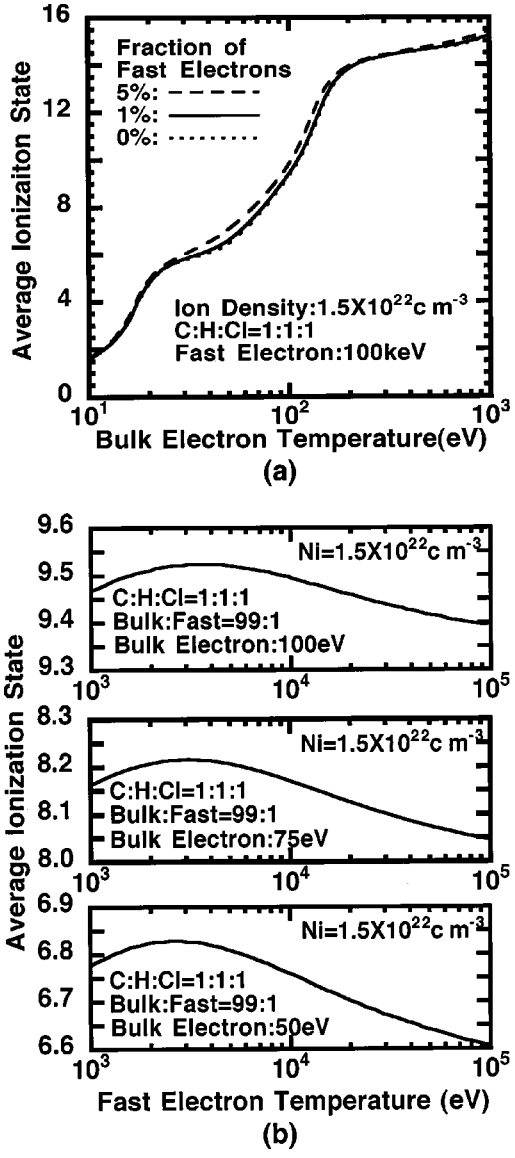


FIG. 4. Average ionization state of partially ionized Cl atoms. (a) $Z_{\mathrm{ave}}^{\mathrm{total}}$ at $T_{\mathrm{fast}}=100$ keV with $h=0$, 0.01, and 0.05. (b) $Z_{\mathrm{ave}}^{\mathrm{total}}$ for $T_{\mathrm{bulk}}=100$, 75, and 50 eV with $h=0.01$.

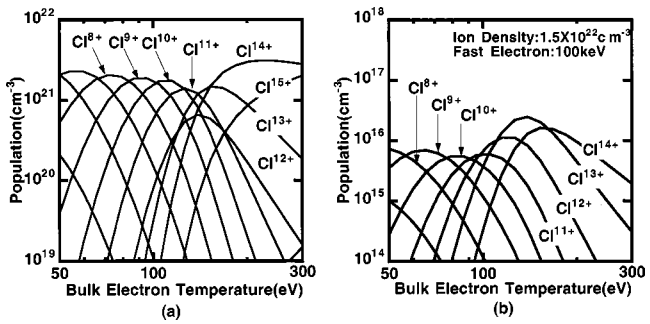


FIG. 5. Population distribution of partially ionized Cl atoms at $T_{\mathrm{fast}}=100$ keV with $h=0.01$. (a) Ground and singly excited states. (b) 1*s*-holed ions.

Figure 4 shows the total average ionization state $Z_{\mathrm{ave}}^{\mathrm{total}}$ of dopant Cl atoms. Plasma is assumed to consist of CHCl. The number of a fraction of fast electrons is 1% of all free electrons. The total ion density $N_i$ is $1.5\times10^{22}$ cm$^{-3}$ corresponding to near solid density. It is seen that the $Z_{\mathrm{ave}}^{\mathrm{total}}$ is strongly affected by bulk-plasma temperature $T_{\mathrm{Bulk}}$, but not by fast-electron properties such as temperature and fraction. As shown in Fig. 4(a), because of the small fraction of fast electrons, its contribution to the average ionization state is small. Useful diagnostic range of the $K\alpha$ emission for Cl atoms derived from our analysis is about $30\ \mathrm{eV}\leqslant T_{\mathrm{bulk}}\leqslant 200$ eV. For $T_{\mathrm{bulk}}\geqslant 200$ eV, the *K*-shell resonance lines and their lithiumlike satellite lines may be more useful for the spectroscopic observation. Figure 4(b) shows $Z_{\mathrm{ave}}^{\mathrm{total}}$ as a function of fast-electron temperature for plausible bulk temperatures. For example, at $T_{\mathrm{bulk}}=75$ eV or 100 eV, the majority of ions are $Cl^{8+}$ or $Cl^{9+}$. Since the corresponding ground states or singly excited states are dominant over the population, the populations of $Cl^{9+}$ $(1s2s^22p^5)$ and $Cl^{10+}$ $(1s2s^22p^4)$ are mainly created by the *K*-shell inner-shell ionization. The *K*-shell inner-shell ionization energy for $Cl^{8+}{:}1s^22s^22p^5\rightarrow Cl^{9+}{:}1s2s^22p^5$, and $Cl^{9+}{:}1s^22s^22p^4\rightarrow Cl^{10+}{:}1s2s^22p^4$ processes are, respectively, about 3053 eV and 3130 eV from the calculation. Thus, the $Z_{\mathrm{ave}}^{\mathrm{total}}$ shows a small peak around this energy range. In the case of $T_{\mathrm{bulk}}=50$ eV, the majority of ions are $Cl^{6+}$ or $Cl^{7+}$, and the corresponding *K*-shell ionization energies are less than those of $Cl^{8+}$ or $Cl^{9+}$. Therefore, the round peak in this curve is located at a little lower temperature than those for $T_{\mathrm{bulk}}=75$ eV and 100 eV.

Figure 5 gives the abundance of each ionization state at $T_{\mathrm{fast}}=100$ keV. The population of 1*s*-holed ions is very small compared with the corresponding ground state and/or singly excited state ions. Actually, the ratio between both of them is at most (1*s*-holed ions)/(ground state and singly excited state ions) $\approx 10^{-5}$, and the charge states of dominant ions in Figs. 5(a) and 5(b) may be related with each other as follows:

$$Z_{\mathrm{ave}}^{\mathrm{total}}\approx Z_{\mathrm{ave}}^{\mathrm{bulk}}\approx Z_{\mathrm{ave}}^{1s\text{-holed}}-1, \tag{11}$$

where $Z_{\mathrm{ave}}^{\mathrm{bulk}}$ means the average ionization state of bulk

plasma and $Z_{\mathrm{ave}}^{1s\text{-holed}}$ is for $1s$-holed ions $N^*(z,1)$. Therefore, it is expected that the $Z_{\mathrm{ave}}^{\mathrm{total}}$ is obtained via the $Z_{\mathrm{ave}}^{1s\text{-holed}}$.

In our present model, only ground states of $1s$-holed ions are included. As long as the fraction of fast electrons is very small compared to that of bulk electrons, the approximation for the $K\alpha$ emission by the product of the rate of the $K$-shell ionization of the ground-state populations and the fluorescence yield, where the ground-state populations are obtained from Eq. (9) without Eq. (10), may work well. Actually, the ionization and/or recombination between the ground states of $1s$-holed ions do not affect the ground-state populations of $1s$-holed ions so much. However, the $K\alpha$ emission from excited states may overlap with those from low-lying atomic states of the next ionization state [18]. When the excited atomic states of $1s$-holed ions are included, not only bound-bound transitions within the same ionization state of $1s$-holed ions but also ionization and/or recombination between excited $1s$-holed ions and ground-state ones of the next ionization state, may affect the population distribution. Equation (11) simply shows the estimation without making any distinction between detailed atomic states. From the viewpoint of the average ionization state, as long as the fraction of fast electrons is small, Eq. (11) may be valid.

To deduce plasma temperature, taking intensity ratios between two $K\alpha$ emissions for different charge states is more convenient. Regarding the role of $K\alpha$ emission from excited states, MacFarlane *et al.* [18] suggested that $K\alpha$ emission from excited states, for example, F-like Al ions [namely, $\mathrm{Al}^{4+}$:$1s2s^22p^53l \rightarrow 1s^22s^22p^43l$ $(l=s,p,d)$] overlapped significantly with those from low-lying states of O-like Al. Although our calculation does not include the $K\alpha$ emission from the corresponding excited states, we will apply our code to deduce bulk-plasma temperature by taking several combinations of intensity ratios between different charge states. The results are described in Sec. V.

In addition, fractional fast electrons in the electron distribution are also important to determine plasma properties. Figure 6 gives sensitivity of the line ratios on the plausible fractions. The solid line shows the comparison between $h=0.05$ and $h=0.01$, and the broken line between $h=0.02$ and $h=0.01$. Here, four $K\alpha$ lines of $\mathrm{Cl}^{10+}$ to $\mathrm{Cl}^{13+}$ are considered. It is found that, even though the fraction of fast electrons is very small, the population of $1s$-holed ions can be noticeably affected, particularly $T_{\mathrm{bulk}} \leqslant 200$ eV. Therefore, explicit derivation of the fast-electron fraction is indispensable.

## V. COMPARISON WITH EXPERIMENTAL RESULTS

The results of model calculation were compared with experimentally obtained Cl $K\alpha$ emission. First, experimental conditions and a typical spectrum are described, then the results are plotted on the curves of line ratios to deduce plasma temperature.

### A. Setup of experiments

Experiments were carried out with the use of Ti:sapphire laser system named T6 at the Institute of Laser Engineering,

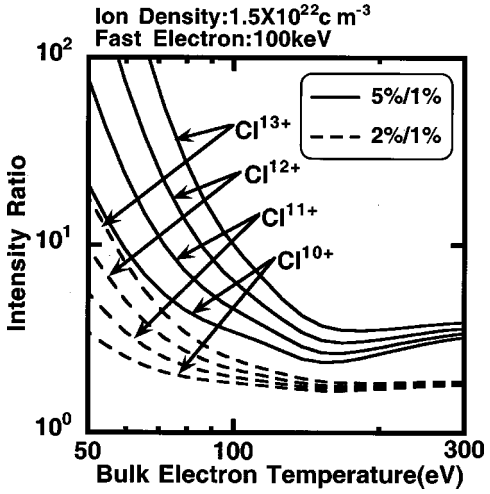


FIG. 6. Intensity ratios of $K\alpha$ emissions from the same ionization states but two different fast-electron fractions $h$ at $T_{\mathrm{fast}}=100$ keV. Solid lines, intensity ratios of the respective lines for $h=0.05$ to $h=0.01$. Broken lines, intensity ratios for $h=0.02$ to $h=0.01$.

Osaka [33]. This laser provides energy of 50 mJ per pulse at the center wavelength λ of 800 nm at a 10 Hz repetition rate. These pulses were focused with an $f/3$ off-axis parabolic mirror onto a target at normal incidence with a focal spot diameter of 15 $\mu$m including 80% of an incident energy. The pulse duration was 130 fs. These conditions yielded a laser intensity of $1.5\times10^{17}$ W/cm$^2$. The target was a 200 $\mu$m thick polyvinylchloride ($C_2H_3Cl$) sheet mounted on a rotating table to provide a fresh surface for every shot. The density of the sheet was 1.4 g/cc. X-ray spectra from the target were observed with a two-dimensionally curved, crystal spectrograph. The bent crystal was a quartz with meridional curvature radius of 200 mm and sagittal curvature radius of 178 mm. It was used in (10-1-1) reflection and set 1162 mm away from the target. The meridional direction includes the dispersion plane. Resultant image magnification was 1/8. X-ray spectra ranging from 2583 to 2883 eV in emission energy were recorded with a cooled, back-illumination charge-coupled device (CCD) detector. Spectral resolution $\epsilon/d\epsilon$ (here $\epsilon$ is the x-ray photon energy) was better than $10^4$. The observation angle was 45° from the target normal. In order to obtain clear signal on CCD, typically $10^4$ shots were needed.

### B. Results and discussions

Figure 7 shows a typical spectrum from the laser produced $C_2H_3Cl$ plasma, and comparison with the code calculation. In Fig. 7(a), it is seen that the $K\alpha$ emissions of $\mathrm{Cl}^{1+}$ $(1s2s^22p^63s^23p^5 \rightarrow 1s^22s^22p^53s^23p^5)$ to $\mathrm{Cl}^{15+}$ $(1s2p \rightarrow 1s^2)$ are lying in the region of about 2600–2800 eV. The $K\alpha$ emissions of $\mathrm{Cl}^{2+}$ to $\mathrm{Cl}^{8+}$ completely overlap with the primary one ($\mathrm{Cl}^{+}$), showing a wide unresolved line-shape feature.

Figures 7(b) and 7(c) show calculated line ratios as functions of bulk-electron temperature for two different $h$'s. Also, experimental line ratios are plotted on the calculated

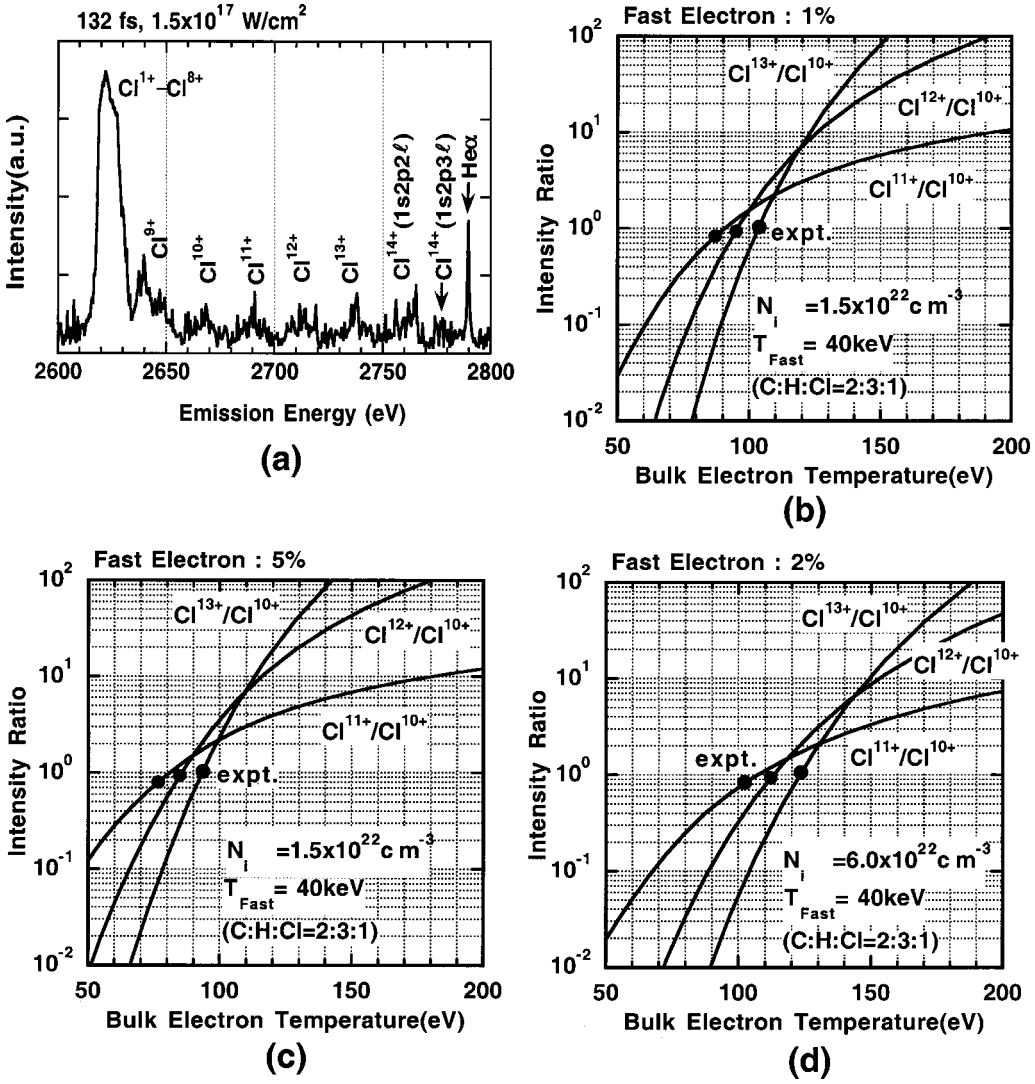


FIG. 7. Time- and space-integrated spectrum obtained from the experiment, and comparison of the result with code calculation. (a) Experimental spectrum. (b) Comparison of the experimental and numerical results for $h=0.01$. (c) Same as (b) but for $h=0.05$. (d) Same as (b) but for $N_i=6.0\times10^{22}$ cm$^{-3}$, and $h=0.02$.

curves. Plasma density $N_i$ is assumed to be $1.5\times10^{22}$ cm$^{-3}$. Due to difficulty in isolation of $Cl^{9+}$ $K\alpha$ line from the integrated primary one ($Cl^{+}-Cl^{8+}$), intensity ratios are taken with respect to the $Cl^{10+}$. According to numerical predictions with particle-in-cell codes [34–36], the fraction of fast electrons is at most a few percent of all free electrons. From Refs. [37,38], the temperature of fast electrons is approximately estimated by the $J\times B$ ponderomotive model: $T_{\rm fast}({\rm keV})\approx m_e c^2[\sqrt{1+7.28\times10^{-19}(I\lambda^2)}-1]$, where $I\lambda^2$ is in units of W cm$^{-2}$ $\mu$m$^2$. Recently, Okihara *et al.* have studied experimentally and numerically the temperature of fast electrons produced by an intense laser pulse with the use of T6 laser system, and obtained a higher temperature than that predicted by the equation [39]. They suggested that this increase may be due to some additional mechanisms like a wakefield acceleration in preformed plasma onto a simple ponderomotive force. According to their result, $T_{\rm fast}$ may be about 40 keV for our experimental condition. By using this $T_{\rm fast}$, average bulk-plasma temperatures for Figs. 7(b) and 7(c) are obtained to be $96\pm8$ eV (for $h=0.01$) and $86\pm8$ eV (for $h=0.05$), respectively. The difference between them appears to be small. However, it may be expected that the determination of a fast-electron fraction is important when an individual line shape of $K\alpha$ emission including corresponding satellite lines has to be taken into consideration. The $K\alpha$ lines from the excited states can overlap with those of the next ionization states [18], and the fractional fast electrons may contribute to, for example, the inner-shell excitations: $1s^22s^22p^N\rightarrow1s2s^22p^Nnl$. Treatment of the excited states is undertaken.

According to the paper recently published by Andiel *et al.* [40], they measured time history of Al $K\alpha$ emission under the same experimental conditions as ours. Despite 150 fs ultrashort pulses at 790 nm, $K\alpha$ emission with a duration of 4 ps was obtained. This evidence may indicate that the effective heating time of background plasma due to fast-electron propagation is close to 4 ps, which is much longer than the pulse width. Therefore, the heating time of several

picoseconds may be regarded as a critical characteristic time that may govern the atomic processes in our experiment. For example, at $N_i = 1.5 \times 10^{22}$ cm$^{-3}$, $T_{\text{fast}} = 40$ keV ($h = 0.01$), and $T_{\text{bulk}} = 100$ eV [this condition is almost same as that of the result from Fig. 7(b)], the atomic transition rates of inner- and/or outer-shell ionizations, radiative and Auger decays for the ground states of $1s$-holed ions are about $10^{10}$–$10^{11}$, $10^{11}$–$10^{12}$, $10^{13}$–$10^{14}$, and $10^{14}$–$10^{15}$ sec$^{-1}$, respectively. The ion density corresponds to near the solid density of a $C_2H_3Cl$ target. From this estimation, it is likely that the inner-shell ionization is much slower than the effective heating time. However, according to the LASNEX simulation done by Guethlein *et al.* [41] under the conditions similar to our case, the plasma density of the heating area was enhanced by a factor of 4 due to shock compression. In addition, there is an uncertainty of the fraction of fast electrons. Considering these facts, the inner-shell ionization rates can be enhanced by about a factor of 10 compared with the case of Fig. 7(b). Then, the resultant effective rates of the inner-shell ionization of the $K$ shell may be comparable with the inverse of the effective heating time of several picoseconds. Therefore, in this case, our CRE solution may be valid. In Fig. 7(d), the corresponding result with $N_i = 6.0 \times 10^{22}$ cm$^{-3}$, and $h = 0.02$ is shown. From Fig. 7(d), the bulk electron temperature is about $111 \pm 10$ eV. The resultant bulk temperatures deduced from Figs. 7(b), 7(c), and 7(d) are almost the same. In the near future, we will justify this hypothesis with the use of a time-dependent rate equation solver.

Regarding depth of the plasma on the target surface, as was noted by many authors [15,41], it was estimated to be at most about 1 $\mu$m. Some advanced experiments are to be done to see the structure of the heat front in a target plasma.

## VI. CONCLUSION

A rate equation solver specified for the analysis of chlorine $K\alpha$ lines has been developed to deduce electron temperature of cold bulk plasma heated by fast electrons. Atomic processes associated with the $K\alpha$ emission are solved under CRE with a bi-Maxwellian temperature distribution. It has been shown that ionization abundance is critically dependent on the cold-electron temperature but not on the fast-electron one. However, in order to deduce the $K\alpha$ emission more quantitatively, explicit consideration of fast electron distribution is found to be of particular importance. To show applicability of the code, chlorine $K\alpha$ to $Cl^{15+}$ He$\alpha$ lines were observed with a 1 TW Ti:sapphire laser system. Comparison of the experimental results with the code prediction infers a plasma temperature of about 100 eV at $1.5 \times 10^{17}$ W/cm$^2$. It is planned to improve the above code in some aspects including (i) treatment of $K\alpha$ emission from excited states, e.g., $Cl^{8+}$:$1s2s^22p^53l$–$Cl^{12+}$:$1s2s^22p3l$, (ii) opacity effect, and (iii) extension to a time-dependent solver. Furthermore, we are planning to carry out some advanced experiments to find a temperature profile in the depth of plasmas. Results will be reported elsewhere.

## ACKNOWLEDGMENTS

The authors acknowledge Dr. R. Kodama, Dr. Y. Kitagawa, and Dr. K. A. Tanaka of the Institute of Laser Engineering, Osaka University for their invaluable support in this work. Also, the authors would like to thank Dr. Y. Sentoku for fruitful discussions, and are grateful to Dr. T. Schlegel for invaluable comments on our manuscript.

[1] C. Rischel, A. Rousse, I. Uschmann, P. Albouy, J. Geindre, P. Audebert, J. Gauthier, E. Förster, J. Martin, and A. Antonetti, Nature (London) **390**, 490 (1997).
[2] A. J. Mackinnon, M. Borghesi, S. Hatchett, M. H. Key, P. K. Patel, H. Campbell, A. Schiavi, R. Snavely, S. C. Wilks, and O. Willi, Phys. Rev. Lett. **86**, 1769 (2001).
[3] M. Tabak, J. Hammer, M. E. Glinsky, W. L. Kruer, S. C. Wilks, J. Woodworth, E. M. Campbell, M. D. Perry, and R. J. Mason, Phys. Plasmas **1**, 1626 (1994).
[4] B. A. Hammel, C. J. Keane, M. D. Cable, D. R. Kania, J. D. Kilkenny, R. W. Lee, and R. Pasha, Phys. Rev. Lett. **70**, 1263 (1993).
[5] C. J. Keane, B. A. Hammel, D. R. Kania, J. D. Kilkenny, R. W. Lee, A. L. Osterheld, L. J. Suter, R. C. Mancini, C. F. Hooper, Jr., and N. D. Delamater, Phys. Fluids B **5**, 3328 (1993).
[6] H. Nishimura, T. Kiso, H. Shiraga, T. Endo, K. Fujita, A. Sunahara, H. Takabe, Y. Kato, and S. Nakai, Phys. Plasmas **2**, 2063 (1995).
[7] T. Kawamura, K. Mima, and F. Koike, J. Phys. Soc. Jpn. **68**, 104 (1999).
[8] T. Kawamura, K. Mima, and F. Koike, Phys. Plasmas **6**, 3658 (1999).
[9] T. Kawamura, K. Mima, and F. Koike, Plasma Phys. Controlled Fusion **43**, 53 (2001).
[10] I. E. Golovkin and R. C. Mancini, J. Quant. Spectrosc. Radiat. Transf. **65**, 273 (2000).
[11] K. B. Wharton, S. P. Hatchett, S. C. Wilks, M. H. Key, J. D. Moody, V. Yanovsky, A. A. Offenberger, B. A. Hammel, M. D. Perry, and C. Joshi, Phys. Rev. Lett. **81**, 822 (1998).
[12] T. A. Hall, S. Ellwi, D. Batani, A. Bernardinello, V. Masella, M. Koenig, A. Benuzzi, J. Krishnan, F. Pisani, A. Djaoui, P. Norreys, D. Neely, S. Rose, M. H. Key, and P. Fews, Phys. Rev. Lett. **81**, 1003 (1998).
[13] C. Chenais-Popovics, C. Fievet, J. P. Geindre, J. C. Gauthier, E. Luc-Koenig, J. F. Wyart, H. Pépin, and M. Chaker, Phys. Rev. A **40**, 3194 (1989).
[14] N. H. Burnett, G. D. Enright, A. Avery, A. Leon, and J. C. Kieffer, Phys. Rev. A **29**, 2294 (1984).
[15] A. Rousse, P. Audebert, J. P. Geindre, F. Falliès, and J. C. Gauthier, Phys. Rev. E **50**, 2200 (1994).
[16] R. Epstein, S. Skupsky, and J. Delettrez, J. Quant. Spectrosc. Radiat. Transf. **35**, 131 (1986).
[17] Y. T. Lee and M. Lamoureux, Phys. Fluids B **5**, 2235 (1993).

[18] J. J. MacFarlane, P. Wang, J. Bailey, T. A. Mehlhorn, R. J. Dukart, and R. C. Mancini, Phys. Rev. E **47**, 2748 (1993).
[19] K. G. Dyall, I. P. Grant, C. T. Johnson, F. A. Parpia, and E. P. Plummer, Comput. Phys. Commun. **55**, 425 (1989).
[20] S. Fritzsche and B. Fricke, Phys. Scr., T **T41**, 45 (1992).
[21] F. B. Rosmej, J. Phys. B **30**, L819 (1997).
[22] F. B. Rosmej, J. Phys. B **33**, L1 (2000).
[23] T. Ditmire, Phys. Rev. E **54**, 6735 (1996).
[24] R. K. Landshoff and J. D. Perez, Phys. Rev. A **13**, 1619 (1976).
[25] D. H. Sampson and L. B. Golden, J. Phys. B **11**, 541 (1978).
[26] L. B. Golden, D. H. Sampson, and K. Omidvar, J. Phys. B **11**, 3235 (1978).
[27] D. L. Moores, L. B. Golden, and D. H. Sampson, J. Phys. B **13**, 385 (1980).
[28] L. B. Golden and D. H. Sampson, J. Phys. B **13**, 2645 (1980).
[29] R. E. H. Clark and D. H. Sampson, J. Phys. B **17**, 3311 (1984).
[30] Y. T. Lee, J. Quant. Spectrosc. Radiat. Transf. **38**, 131 (1987).
[31] F. Perrot, Phys. Scr. **39**, 332 (1989).
[32] H. A. Bethe and E. E. Salpeter, *Quantum Mechanics of One- and Two-Electron Atoms* (Plenum, New York, 1977).
[33] H. Schillinger, S. Sakabe, T. Kuge, H. Ueyama, T. Urano, S. Kawato, M. Hashida, K. Shimizu, J. Kou, and Y. Izawa, Rev. Laser Eng. **25**, 890 (1997).
[34] Y. Sentoku, K. Mima, T. Taguchi, S. Miyamoto, and Y. Kishimoto, Phys. Plasmas **5**, 4366 (1998).
[35] Y. Sentoku, K. Mima, S. Kojima, and H. Ruhl, Phys. Plasmas **7**, 689 (2000).
[36] Y. Sentoku (private communication).
[37] S. C. Wilks, W. L. Kruer, M. Tabak, and A. B. Langdon, Phys. Rev. Lett. **69**, 1383 (1992).
[38] T. Feurer, W. Theobald, R. Sauerbrey, I. Uschmann, D. Altenbernd, U. Teubner, P. Gibbon, E. Förster, G. Malka, and J. L. Miquel, Phys. Rev. E **56**, 4608 (1997).
[39] S. Okihara, Y. Sentoku, K. Sueda, S. Shimizu, F. Sato, N. Miyanaga, K. Mima, Y. Izawa, T. Iida, and S. Sakabe, J. Nucl. Sci. Technol. **39**, 1 (2002).
[40] U. Andiel, K. Eidmann, K. Witte, I. Uschmann, and E. Förster, Appl. Phys. Lett. **80**, 198 (2002).
[41] G. Guethlein, M. E. Foord, and D. Price, Phys. Rev. Lett. **77**, 1055 (1996).